REPORT DOCUMENTATION PAGE	*Form Approved* *OMB No. 0704-0188*

1. REPORT DATE *(DD-MM-YYYY)*	2. REPORT TYPE	3. DATES COVERED *(From - To)*
09-10-2009	Journal Article	

4. TITLE AND SUBTITLE	
A Simple Underwater Imaging Model	5a. CONTRACT NUMBER
	5b. GRANT NUMBER
	5c. PROGRAM ELEMENT NUMBER 0602782N
6. AUTHOR(S) Weilin Hou	5d. PROJECT NUMBER
	5e. TASK NUMBER
	5f. WORK UNIT NUMBER 73-6369-09-5

7. PERFORMING ORGANIZATION NAME(S) AND ADDRESS(ES)	8. PERFORMING ORGANIZATION REPORT NUMBER
Naval Research Laboratory Oceanography Division Stennis Space Center, MS 39529-5004	NRL/JA/7330-09-9200

9. SPONSORING/MONITORING AGENCY NAME(S) AND ADDRESS(ES)	10. SPONSOR/MONITOR'S ACRONYM(S)
Office of Naval Research 800 N. Quincy St. Arlington, VA 22217-5660	ONR
	11. SPONSOR/MONITOR'S REPORT NUMBER(S)

12. DISTRIBUTION/AVAILABILITY STATEMENT

Approved for public release, distribution is unlimited.

20091021252

13. SUPPLEMENTARY NOTES

14. ABSTRACT

It is commonly known that underwater imaging is hindered by both absorption and scattering by particles of various origins. However, evidence also indicates that the turbulence in natural underwater environments can cause severe image-quality degradation. A model is presented to include the effects of both particle and turbulence on underwater optical imaging through optical transfer functions to help quantify the limiting factors under different circumstances. The model utilizes Kolmogorov-type index of refraction power spectra found in the ocean, along with field examples, to demonstrate that optical turbulence can limit imaging resolution by affecting high spatial frequencies. The effects of the path radiance are also discussed.

15. SUBJECT TERMS

16. SECURITY CLASSIFICATION OF: a. REPORT	b. ABSTRACT	c. THIS PAGE	17. LIMITATION OF ABSTRACT	18. NUMBER OF PAGES	19a. NAME OF RESPONSIBLE PERSON
Unclassified	Unclassified	Unclassified	UL	3	Weilin Hou
					19b. TELEPHONE NUMBER *(Include area code)* 228-688-5257

A simple underwater imaging model

Weilin (Will) Hou

Naval Research Laboratory, 1009 Balch Boulevard, Stennis Space Center, Mississippi 39529, USA (hou@nrlssc.navy.mil)

Received May 5, 2009; revised July 22, 2009; accepted July 31, 2009; posted August 17, 2009 (Doc. ID 111008); published August 31, 2009

It is commonly known that underwater imaging is hindered by both absorption and scattering by particles of various origins. However, evidence also indicates that the turbulence in natural underwater environments can cause severe image-quality degradation. A model is presented to include the effects of both particle and turbulence on underwater optical imaging through optical transfer functions to help quantify the limiting factors under different circumstances. The model utilizes Kolmogorov-type index of refraction power spectra found in the ocean, along with field examples, to demonstrate that optical turbulence can limit imaging resolution by affecting high spatial frequencies. The effects of the path radiance are also discussed.

OCIS codes: 010.4450, 010.7060, 010.7295.

Underwater imaging poses significant challenges at extended ranges when compared with similar situations in the air. Even in the clearest ocean waters, visibility range at best is on the order of tens of meters, while the visibility in air can be on the order of miles under optimal conditions. This significant reduction in range is caused by the absorbing and scattering nature of the medium, which is the water itself, and constituents within, such as particles of various origins, including algal cells, detritus, sediments, plankton, and even bubbles near the surface. Little attention has been paid to the effects of turbulent flows on imaging outcomes, despite evidence suggesting that the optical turbulence can be a limiting factor under certain conditions [1,2]. Overcoming such challenges to increase both the reach and the resolution is of vital importance to military and civilian applications. It is imperative to establish a good understanding about the limiting factors under different conditions.

In underwater imaging, particle scattering and path radiance are commonly known dominant factors in image contrast reduction. Although it is less intuitive than the star twinkling caused by air movements, the optical turbulence has been shown to limit system performance in natural waters [1]. Results developed in previous atmosphere research [3–6] are used with modifications to reflect in-water optical conditions. Key steps and assumptions are also outlined below for convenience and assessing the limitations of the theory. The optical turbulence in the ocean is primarily caused by the index-of-refraction (IOR) variation as functions of the temperature and salinity. It has been shown that IOR fluctuations can be expressed as linear combinations of individual elements, in terms of both the power spectrum and the structure function [7]. Following the Kolmogorov model [3], for a fully developed turbulent flow, under the inertial subregime, $2\pi/L_0<\kappa<2\pi/l_0$ (κ is the wavenumber corresponding to eddy scales; L_0 and l_0 denote outer and inner scale, respectively [4]), the power spectral density of the IOR of the ocean waters over the imaging range (r) can be expressed in the form of [7,8]

$$\Phi_n^K(\kappa,r)=K_3\kappa^{-11/3}, \tag{1}$$

where $K_3=B_1\chi\varepsilon^{-1/3}$, and it reflects the 3D optical turbulence strength. B_1 is a constant and is assumed to be of order of unity [8]. ε is the kinetic energy dissipation rate, which typically ranges from 10^{-3} to 10^{-11} $m^2\,s^{-3}$ in natural waters. χ relates to the dissipation rate of temperature or salinity variances [8] and ranges from 10^{-2} to 10^{-9} $C^2\,s^{-1}$ and 10^{-4} to 10^{-11} $psu^2\,s^{-1}$ (psu, practical salinity unit), respectively [9,10]. It is apparent that the above equation has the usual Kolmogorov form found in atmospheric studies as $\Phi_n^K(\kappa,r)=0.033C_n^2(r)\kappa^{-11/3}$ [3–5], where again the superscript K denotes Kolmogorov spectra. C_n^2 is the structure constant of the IOR fluctuations, which describes the optical turbulence strength at a distance r from the pupil plane. K_3 is equivalent of C_n^2, by a constant, and ranges from 10^{-8} to 10^2 in the ocean. The above scalar relationship implies that the turbulence in water is considered statistically isotropic, homogenous, and wide-sense stationary (WSS) such that spatial autocorrelation function depends only on relative positions. It is important to recall that not all turbulent flows can be described by the above spectra [4,7].

It is commonly known that spatial coherence functions between optical fields of any two points can be used to describe the irradiance distribution of the source image or object [5,11]. Using the Wiener–Khinchin theorem [5], the power spectrum (1) is related to the spatial autocorrelation of IOR, which itself is directly linked to the structure function of IOR. Combined, the optical transfer function can be shown as the equivalent to the spatial correlation function on the pupil screen. For a time-varying correlation function under WSS conditions, its ensemble average can be related to the spatial phase-structure function such that the optical transfer function (OTF) of a general incoherent object can be expressed following the approach by Fried [4,6]. The time-averaged, or long exposure (LE) OTF of the optical turbulence in underwater environments takes the form

$$\mathrm{OTF}_{\mathrm{LE}}(f) = \exp\left[-3.44\left(\frac{\bar{\lambda} d_i f}{r_0}\right)^{5/3}\right], \tag{2}$$

where $\bar{\lambda}$ is the mean wavelength (530 nm for typical underwater transmissions [12]). d_i is the distance between the pupil plane and the detector; f is the spatial frequency on the pupil plane in units of inverse length. r_0 is the so-called seeing or Fried parameter, defined over the propagation distance r as

$$r_0 = 0.185\left[\frac{4\pi^2}{k^2\int_0^r \mathrm{d}z C_n^2(z)}\right]^{3/5}, \tag{3}$$

and $k=2\pi/\bar{\lambda}$. If we consider the optical turbulence throughout the imaging range to be homogenous and isotropic, it can be described by a constant independent of distance to the pupil plane, $C_n^2(z)=C_w^2$, so that $\int_0^r \mathrm{d}z C_n^2(z)=rC_w^2$, we have

$$r_0 = 0.185\left[\frac{4\pi^2}{k^2C_w^2}\right]^{3/5}, \quad r^{-3/5} = 0.185\left[\frac{0.132\pi^2}{k^2K_3}\right]^{3/5},$$

$$r^{-3/5} = R_0 r^{-3/5}, \tag{4}$$

which is a function of the range (r). R_0 will be referred to as the characteristic seeing parameter and denotes the seeing at the unit distance (1 m). It is important to notice that the underwater seeing parameter reduces over range at a rate close to the square root of r, implying fast rolloff of high spatial frequencies at extended ranges. Consequently, the time-averaged $\mathrm{OTF}_{\mathrm{tur}}$ is also a function of the range r,

$$\mathrm{OTF}_{\mathrm{tur}}(\psi,r) = \exp\left[-3.44\left(\frac{\bar{\lambda}}{R_0}\right)^{5/3}\psi^{5/3}r\right] = \exp(-S_n\psi^{5/3}r), \tag{5}$$

where $S_n=3.44(\bar{\lambda}/R_0)^{5/3}=1736K_3\bar{\lambda}^{1/3}$ and the angular spatial frequency $\psi=d_i f$. The average wavelength is used here, as the phase shift caused by the IOR variation due to the temperature or salinity is not primarily wavelength dependent.

Another factor that affects underwater imaging is the path radiance. This effect can be quantified with a simple setup that produces generalized solutions. If we assume that one transferred frequency component (the sinusoid in Fig. 1) has amplitude x above the mean, which is valued at 1, it is easy to see that between the original amplitude (1) and the current value (x), the modulation function is

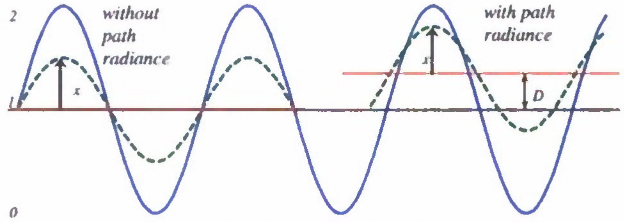

Fig. 1. (Color online) A sinusoid (single frequency) is used to illustrate effects of the path radiance on the modulation transfer. The left side shows the case of the initial wave form (solid) with an amplitude of 1 (varies between 0 and 2) and the wave form after the transmission (dashed) with an amplitude of x from the mean, where x also equals the modulation (see text); the normalized path radiance (D) is shown to elevate the previous wave form by $1/(D+1)$ for all spatial frequencies.

$$M_{\mathrm{orig}} = \frac{I_{\max}-I_{\min}}{I_{\max}+I_{\min}} = \frac{1+x-(1-x)}{1+x+1-x} = x. \tag{6}$$

Adding the normalized radiance D received by the detector, assuming nonsaturation for simplicity, the modulation after the effects of the path radiance now becomes

$$M' = \frac{I_{\max}-I_{\min}}{I_{\max}+I_{\min}} = \frac{1+x+D-(1-x+D)}{1+x+D+1-x+D} = M_{\mathrm{orig}}\left(\frac{1}{1+D}\right) = M_{\mathrm{orig}}\mathrm{MTF}_{\mathrm{path}}. \tag{7}$$

The result shows that the path radiance affects all frequencies equally and that the net effect is a shift of the entire modulation transfer curve; thus it does not affect relative contributions between the turbulence and particles. Naturally, at $D=0$ (no path radiance), Eq. (7) shows $\mathrm{MTF}_{\mathrm{path}}=1$ (MTF is the modulation transfer function). One can easily see $\mathrm{MTF}_{\mathrm{path}} \to 0$ with a large D, describing the saturation by ambient lights, which limits all frequencies. This is in general agreement with earlier results [13] but without any specific illumination limitation. As the ambient light is incoherent in nature, the MTF can be considered the same as the OTF.

Considering that random phase changes of a wavefront can be described independently as a thin screen that exists only when the turbulence exists, the resting or averaged OTF will be that of particles only. This assures linearity of system components, which allows the cascading of OTFs in the frequency domain [11]. From this, we can arrive at a simple underwater imaging equation that accounts for the particle [12], the path radiance, and the turbulence scattering,

$$\mathrm{OTF}(\psi,r)_{\mathrm{total}} = \mathrm{OTF}(\psi,r)_{\mathrm{path}}\mathrm{OTF}(\psi,r)_{\mathrm{par}}\mathrm{OTF}(\psi,r)_{\mathrm{tur}} = \left(\frac{1}{1+D}\right)\exp\left[-cr+br\left(\frac{1-e^{-2\pi\theta_0\psi}}{2\pi\theta_0\psi}\right)\right] \times\exp(-S_n\psi^{5/3}r)$$

$$= \left(\frac{1}{1+D}\right)\exp\left\{-\left[c - b\left(\frac{1-e^{-2\pi\theta_0\psi}}{2\pi\theta_0\psi}\right) + S_n\psi^{5/3}\right]r\right\}, \quad (8)$$

where θ_0 relates to the mean scattering. c and a are the beam attenuation and absorption coefficients, respectively. It is worth pointing out that the OTF_{par} can take many different forms, depending on how the scattering phase structure is incorporated [14].

The simple underwater imaging model, Eq. (8), accounts for scattering from particles and the optical turbulence as well as the path radiance in the underwater environments. The primary aim of the model is to determine the relative contributions, which is essential in assessing the limits of conventional passive systems under different underwater conditions. The model has been applied successfully to explain discrepancies between diver observations and model outputs, particularly involving high-frequency components [15]. Selected optical conditions corresponding to the clear water ($c=0.3\ \mathrm{m}^{-1}$), strong turbulent environments ($\varepsilon=10^{-3}\sim10^{-5}$, $\chi=10^{-10}\sim10^{-11}$, $R_0=0.002\sim0.004$) are used to illustrate the relative effects of particle and turbulence scattering on imaging transmissions, shown in Fig. 2. We see that the turbulence scattering reduces imaging details rapidly, especially with increased path lengths. It has limited effects on low-frequency components when compared with particle scattering, even in clear waters. Equation (8) and Fig. 2 also help to explain why Mertens reported no frequency higher than 1 cycle/mrad observed in the field, which puzzled Duntley [16], as at such high spatial frequencies, the relative contrast decreases rather rapidly towards zero. Lastly, this model helps to explain the extreme turbulence situation observed by Gilbert and Honey [1]. If one converts the standard United States Air Force (USAF) resolution chart [1] line pairs to spatial frequencies, the first blurred group (−1) corresponds to 650 cycles/rad. Applying Eq. (8) with $c=0.3$, $R_0=0.0005$, which corresponds to a clear water, strong turbulence condition ($\varepsilon=10^{-5}$, $\chi=10^{-11}$), one can see that the total contrast easily decreases to less than 2% within the imaging range, which explains the complete disappearance as reported [1].

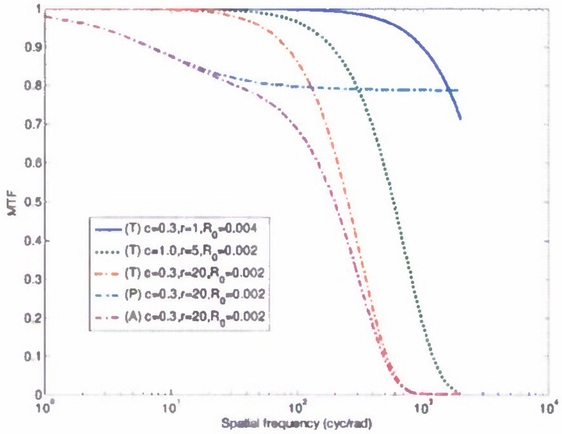

Fig. 2. (Color online) Comparison of relative contributions under different conditions: (T), the OTF contribution from the turbulence; (P), the particle scattering contribution; (A), all combined contributions. Figure legends under corresponding labels indicate attenuation coefficients, imaging ranges, and seeing parameters respectively (in m^{-1}, m and m). The single-scattering albedo of all curves is assumed a constant (0.8). The last three curves in the legend are contributions from the particle, the turbulence, and combined (from top to bottom) under the same optical conditions. No path radiance was included ($D=0$).

Equation (8) reflects the optical properties of the medium under incoherent cases. Since the coherent cutoff frequency is often less [5], this can be used only as a crude estimate under coherent cases. Further, it includes neither effects of the backscattering nor cases with saturations that only further degrade the MTF. This approach is not directly applicable to active systems, such as those gated and modulated, although modifications can be made to reflect impacts on shorter integration time to obtain system limitations similar to approach used in [6].

The author thanks the Naval Research Laboratory for continuous support through project 73-6369. The author also thanks W. McBride and A. Weidemann, and reviewers for suggestions.

References

1. G. D. Gilbert and R. C. Honey, in *Underwater Photo-Optical Instrumentation Applications* (SPIE, 1972), pp. 49–55.
2. D. J. Bogucki, J. A. Domaradzki, R. E. Ecke, and C. R. Truman, Appl. Opt. **43**, 5662 (2004).
3. V. I. Tatarskii, *Wave Propagation in a Turbulent Medium* (Dover, 1967).
4. M. C. Roggemann and B. M. Welsh, *Imaging through Turbulence* (CRC Press, 1996).
5. J. W. Goodman, *Statistical Optics* (John Wiley & Sons, 1985).
6. D. L. Fried, J. Opt. Soc. Am. **56**, 1372 (1966).
7. A. S. Fields, Rep. 3577, Naval Ship Research and Development Center, 1972.
8. G. K. Batchelor, J. Fluid Mech. **5**, 113 (1959).
9. J. A. Domaradzki *Light Scattering Induced by Turbulence Flow: a Numerical Study* (U. Southern California, 1997), p. 65.
10. J. D. Nash and J. N. Moum, J. Atmos. Ocean. Technol. **16**, 263 (1999).
11. J. W. Goodman, *Introduction to Fourier Optics* (Roberts & Company, 2005).
12. W. Hou, Z. Lee, and A. Weidemann, Opt. Express **15**, 2791 (2007).
13. N. Kopeika, Opt. Eng. **26**, 1146 (1987).
14. W. Hou, D. Gray, A. Weidemann, and R. Arnone, Opt. Express **16**, 9958 (2008).
15. W. Hou and A. Weidemann, Proc. SPIE **7317**, 731701 (2009).
16. S. Q. Duntley, in *Optical Aspects of Oceanography*, N. G. Jerlov and E. S. Nielsen, eds. (Academic, 1974).